METOP-B IASI DATA QUALITY AND IMPACT ASSESSMENT

James Cameron, James Cotton, Richard Marriott

Met Office, FitzRoy Road, Exeter, EX1 3PB, United Kingdom

Abstract

The quality of MetOp-B IASI data is assessed by comparing statistics of observed minus forecast background brightness temperature for MetOp-B IASI to those of MetOp-A IASI. It is found that the bias of MetOp-B IASI is the same as that of MetOp-A IASI to less than 0.1K. The Standard deviation of observed minus background is 10-15% less for MetOp-B than for MetOp-A in some channels. Inter-FOV biases are smaller for MetOp-B than for MetOp-A.

The impact on forecasts from assimilating MetOp-B IASI has been tested for two different seasons. Assimilating MetOp-B IASI improves the forecasts in both cases. There is a 20% increase in the number of IASI observations assimilated. The data coverage is improved and the system will be more robust to interruptions in the flow of data. A forecast sensitivity experiment for the period 23 March–25 April 2013 indicates that the impact per observation for MetOp-B IASI is very similar to that of MetOp-A IASI, providing evidence that MetOp-B IASI is delivering the expected impact.

INTRODUCTION

MetOp-B IASI data has been operationally assimilated in the Met Office global model since 19 February 2013. The decision to begin assimilation was based on a positive assessment of the data quality (Cameron, 2013a). The data quality assessment has been repeated using IASI data from 1-15 June 2013 and is discussed in the following section. Observing system experiments have been performed to assess the impact of assimilating MetOp-B IASI. The operational set-up and the impact from assimilating MetOp-B IASI are also discussed before concluding.

DATA QUALITY

To examine differences in the performance of MetOp-A and MetOp-B IASI the fit of IASI observations to simulated observations, modelled from the Met Office forecast background fields using RTTOV-9, were compared for the period 1-15 June 2013. EUMETCast distributed observations were processed through the Met Office's Observation Processing System (OPS) to produce the required statistics. The OPS is used for quality control and to fit parameters that are not present in the 4D-Var control vector. Parameters fitted in the OPS are skin temperature, cloud top height and cloud fraction. Only channels that peak well above the cloud top (channels where the integrated temperature Jacobian below the cloud top is less than 10% of the total integrated temperature Jacobian) or where the fitted cloud fraction is less than 5% are selected for assimilation. In this comparison the same bias correction, derived from MetOp-A data from the period 17 May–11 June, was applied to both MetOp-A and MetOp-B data.

The upper plot in figure 1 shows the mean raw (not bias corrected) observed brightness temperature versus wavenumber for MetOp-A (black) and MetOp-B (red) for the period 1-15 June 2013 for cloud-free observations over the sea, where cloud-free means a fitted cloud fraction of less than 5%. The two lines very nearly overlap so that only MetOp-B is visible. Only the 314 channels received via EUMETCAST are plotted. The lower plot in the same figures shows the difference between the mean MetOp-B and MetOp-A brightness temperatures. The differences are typically less than 0.1K.

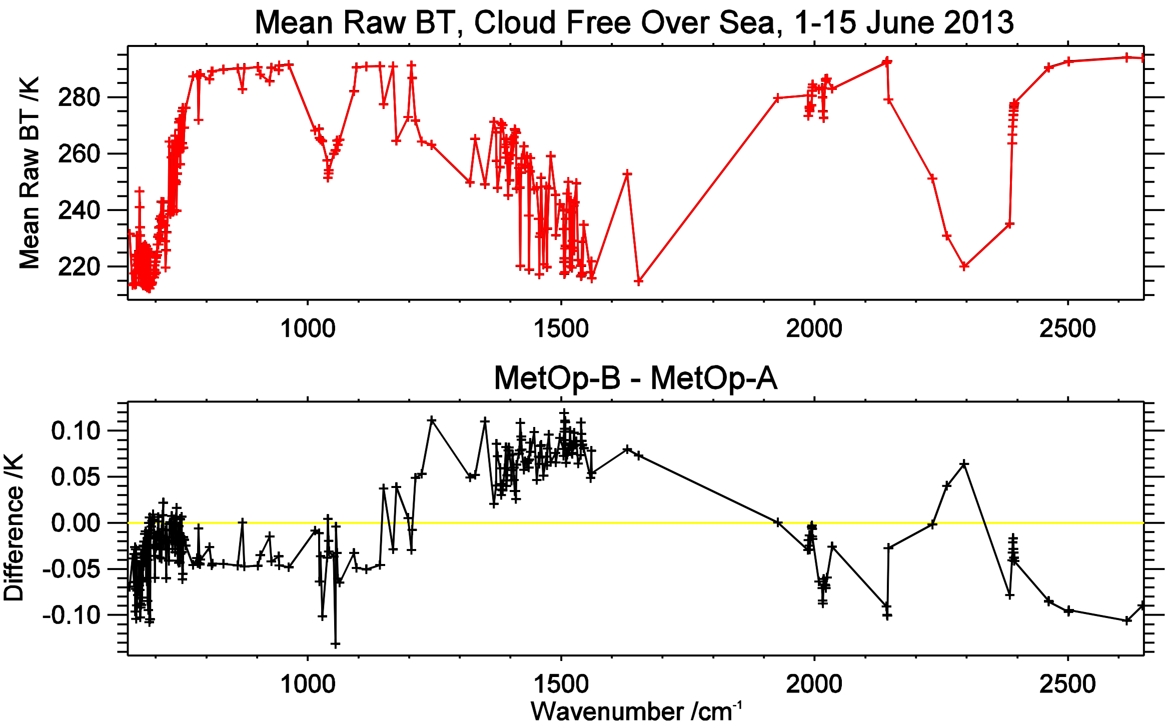

Figure 1: **The upper plot shows the average raw brightness temperature of cloud-free observations over the sea for MeOp-A IASI (black) and MetOp-B IASI (red). Only the 314 IASI channels distributed via EUMETCast are shown. The red MetOp-B line almost completely covers the black MetOp-A line. The lower plot shows the difference between the two lines in the upper plot.**

Figure 2 is a similar plot to figure 1 but shows the mean bias corrected minus forecast background brightness temperatures for MetOp-A and MetOp-B IASI. There are strong residual biases for the Q-branch (662.75 cm^{-1}), the ozone channels (1014.50–1062.50 cm^{-1}) and also for many of the water vapour sensitive channels (around 1500cm^{-1}). Despite these residual biases, it can be seen from the lower plot in figure 2 that the bias is very similar for MetOp-A and MetOp-B, and is typically less than 0.05K.

Figure 3 shows the standard deviation of the bias corrected minus forecast background brightness temperatures for MetOp-A and MetOp-B and the fractional difference between MetOp-B and MetOp-A. It can be seen that the standard deviation of the lowest frequency channels are 10-15% lower for MetOp-B than for MetOp-A. Some of the high frequency channels also have a lower standard deviation. These high and low frequency channels are well modelled and it is highly likely that this difference is due to a lower instrument noise at these frequencies. The fractional difference is much smaller for the water vapour sensitive channels around 1500 cm^{-1}. For these channels the standard deviation will be dominated by forecast error rather than instrument noise.

Figures 4 shows histograms of bias corrected minus background brightness temperature for 6 channels. There is a cold tail on the 901.50cm^{-1} window channel histogram, but it is a logarithmic scale and the tail is present for both MetOp-A and MetOp-B. The most visible difference between MetOp-A and MetOp-B is for the long-wavelength stratospheric temperature sounding channel where the mean bias corrected minus background is slightly less for MetOp-B and the distribution is narrower. This is consistent with the differences shown in figures 2 and 3.

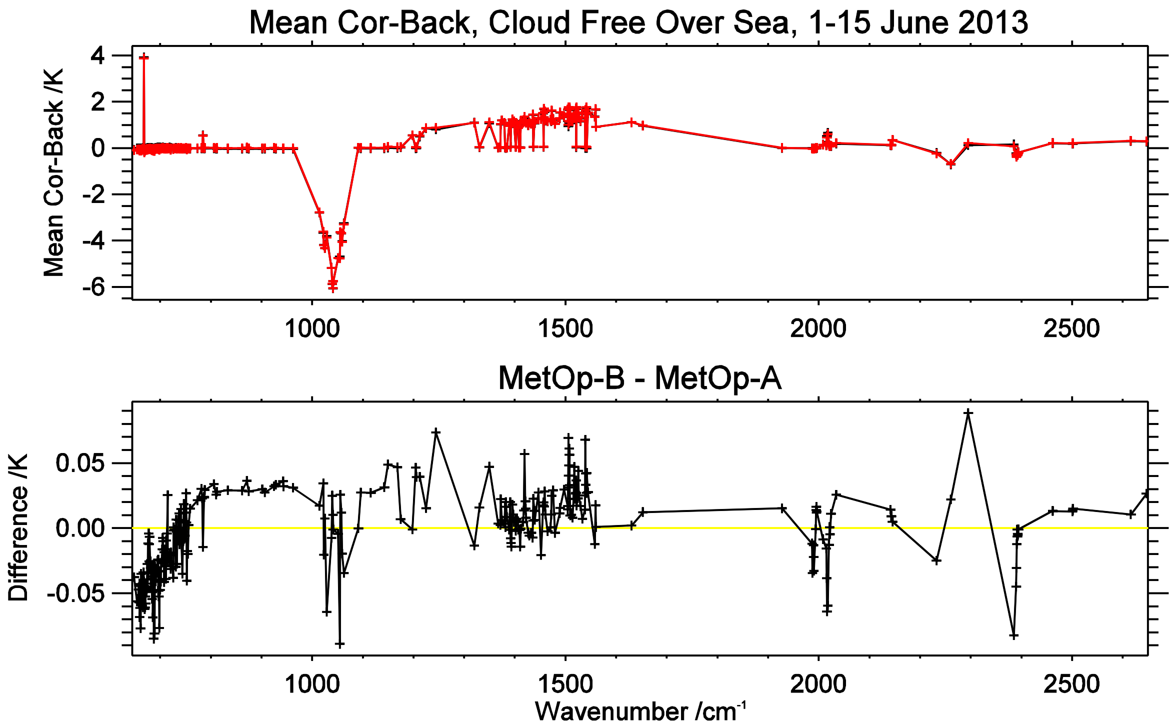

Figure 2: **The mean bias corrected observed brightness temperature minus forecast background for cloud-free observations over the sea for MetOp-A IASI (black) and MetOp-B IASI (red). The difference is shown in the lower plot.**

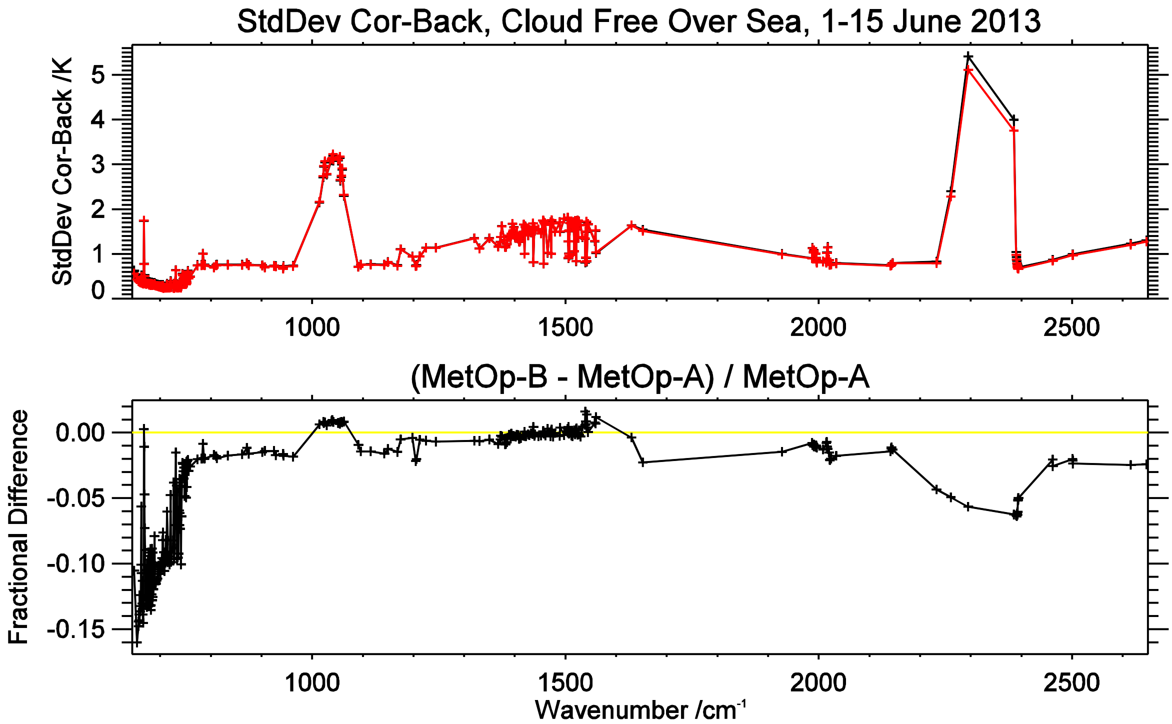

Figure 3: **The standard deviation of bias corrected observed brightness temperature minus forecast background of cloud-free observations over the sea for MetOp-A IASI (black) and MetOp-B IASI (red). The fractional difference is shown in the lower plot.**

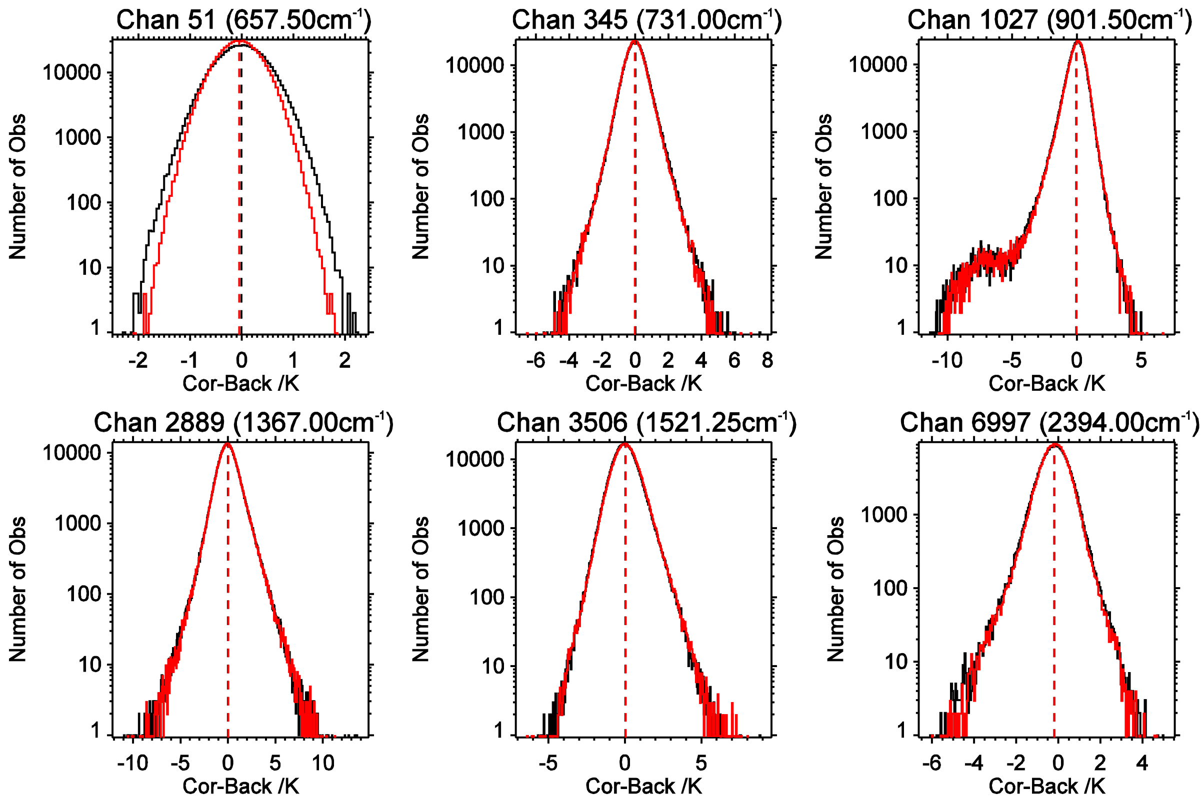

Figure 4: **Histograms of bias corrected observed minus forecast background brightness temperatures for 6 IASI channels. The channels are a long-wavelength stratospheric temperature channel, a mid-tropospheric temperature channel, a window channel, low peaking and high peaking water vapour channels and a short-wavelength window channel. MetOp-A data is plotted in black and MetOp-B in red.**

FOV differences

IASI measures the radiances for 4 fields of view simultaneously. In the OPS these fields of view are referred to as pixels and are numbered 1-4. The bias of each of these pixels could in principle be different, although in practise the differences are small for MetOp-A. The Met Office bias correction scheme currently applies the same bias correction to all pixels.

Figure 5 shows the difference between the mean bias corrected minus forecast background for each pixel individually and the mean for all four pixels together for both MetOp-A (top plot) and MetOp-B (bottom plot). The pixel biases are more tightly grouped for MetOp-B than for MetOp-A. Figure 6 shows a similar plot for the standard deviation of the bias corrected minus forecast background brightness temperatures. In MetOp-B the differences are largest in those channels that have the largest standard deviations (ozone, water vapour, and a few high-peaking short wave channels). Overall the performance of the 4 pixels appears to be at least as well matched on MetOp-B as they are on MetOp-A.

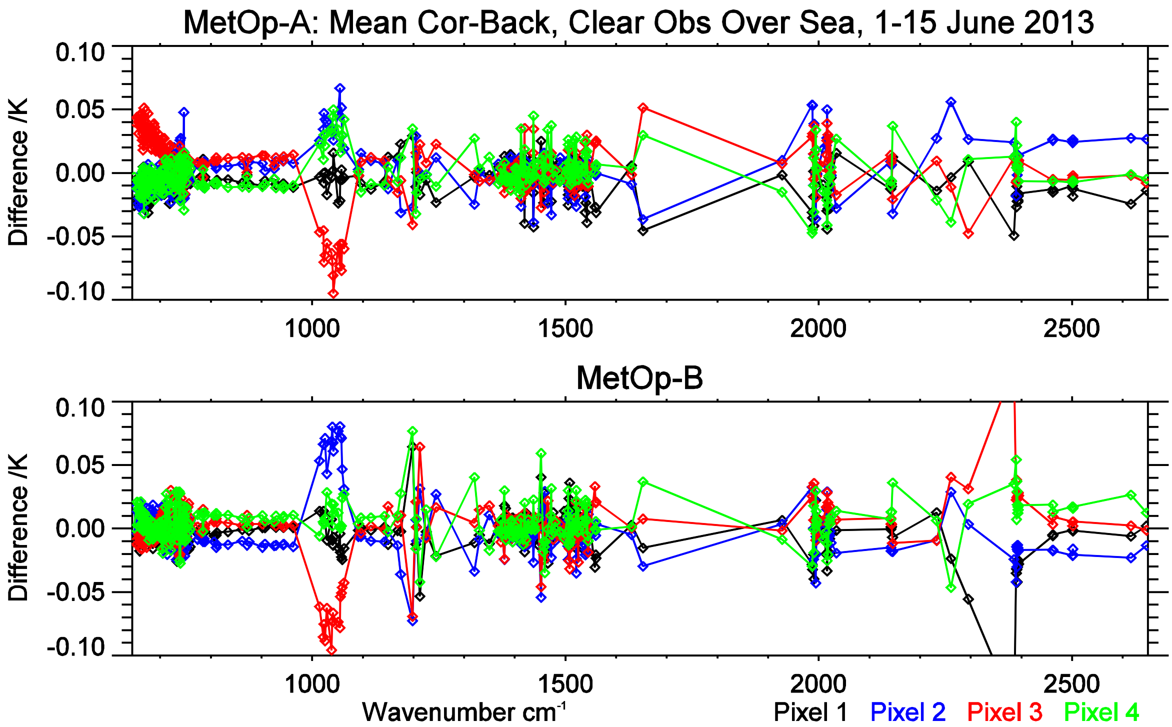

Figure 5: **The difference between the mean bias corrected minus forecast background of each pixel and the mean bias corrected minus forecast background of all four pixels. MetOp-A is shown in the upper plot and MetOp-B below.**

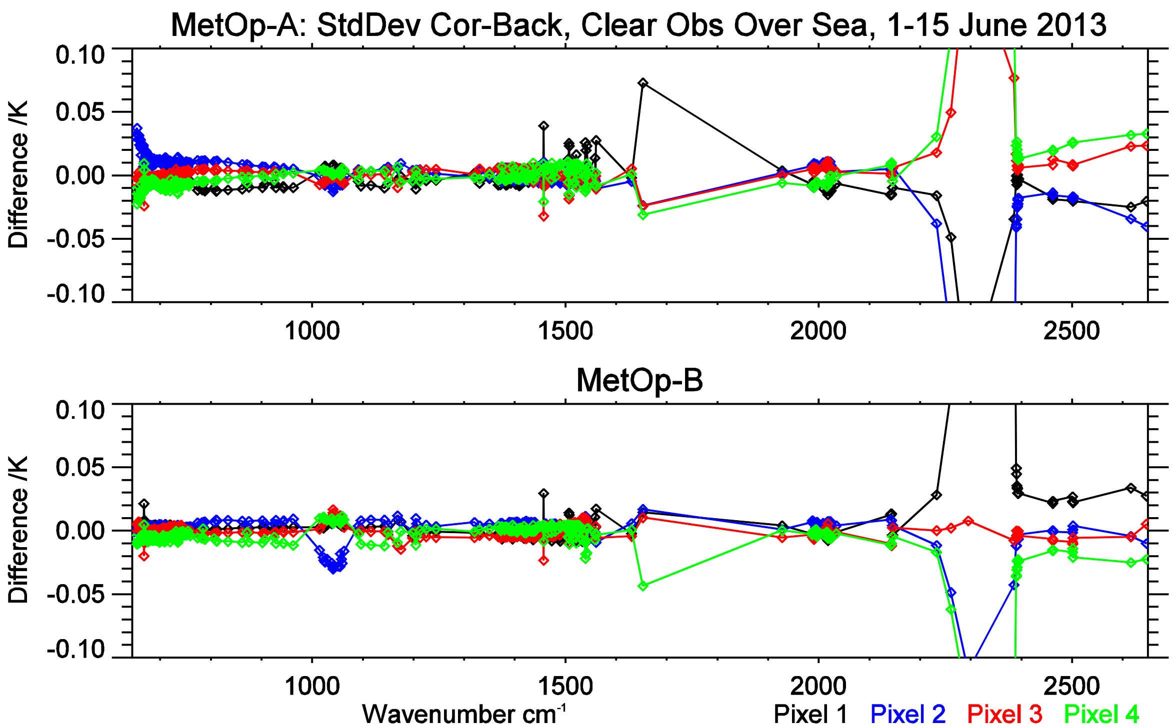

Figure 6: **The difference between the standard deviation of bias corrected minus forecast background of each pixel and the standard deviation of bias corrected minus forecast background including all four pixels. MetOp-A is shown in the upper plot and MetOp-B below. 2 or 3 of the high-peaking short-wave channels extend to beyond the scale shown but none go beyond ±0.4K.**

IMPACT ASSESSMENT

Operational set-up

MetOp-B IASI observations have been operationally assimilated in the Met Office global model since 19 February 2013. The channel selection and observation error used for the processing of MetOp-B IASI are the same as those for MetOp-A IASI. At the Met Office, IASI observations are first processed through the Observation Processing System (OPS) before the data is thinned and the remaining observations assimilated in VAR. The data is currently thinned to 154km in the tropics and 125km in the extra-tropics. At the time of its introduction to operations, MetOp-B was still in the calibration and validation phase and no forecast impact studies had been carried out. Accordingly it was decided to give MetOp-A IASI priority in the data thinning. Figure 7 shows typical data coverage for a 6 hour data assimilation time window. The addition of MetOp-B IASI data results in an approximately 20% increase in the number of IASI observations assimilated. The MetOp-B data fills the gaps between MetOp-A swaths, giving more uniform coverage. Since the gaps between the swaths are wider in the tropics, the latitudinal distribution of assimilated observations will not be quite the same for MetOp-B as for MetOp-A. Assimilating two IASI instruments adds to system robustness because if one instrument drops out briefly then observations from the other instrument will provide continuity.

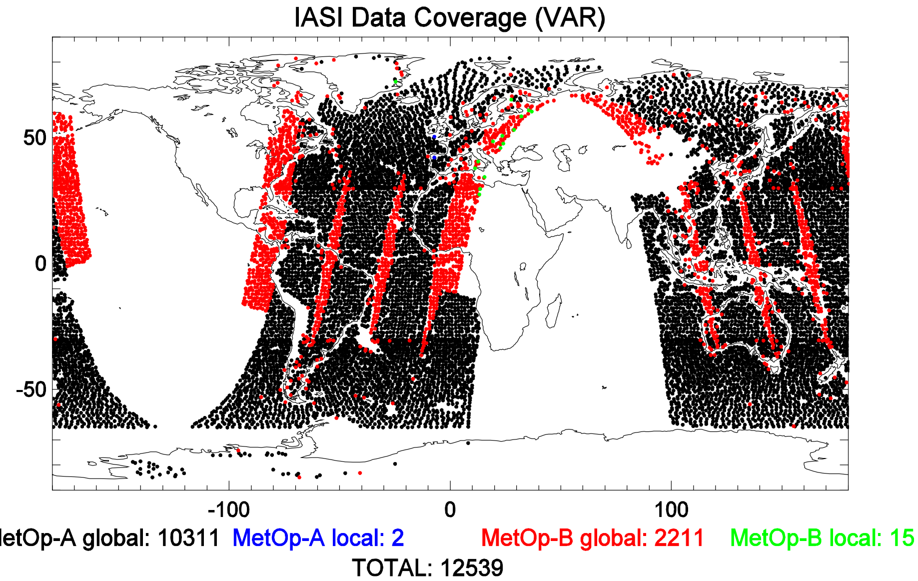

Figure 7: **The distribution of IASI observations passed to VAR for a typical data assimilation cycle. MetOp-A observations are shown in black and MetOp-B observations in red. Locally received MetOp-A and MetOp-B IASI data are shown in blue and green respectively. Locally received observations have the lowest priority in the data thinning.**

Observing System Experiments

Two sets of observing system experiments have been carried out using MetOp-B IASI data. The first set of experiments ran over the period 1 February–25 March 2013. MetOp-B IASI was still in the calibration and validation phase at this time and consequently there were a number of data outages. There was also a calibration update to MetOp-B IASI on 14 March. The second trial period was 1 July–15 August 2013. The impact of adding MetOp-B IASI to a system that includes MetOp-A IASI and MetOp-B ATOVS, ASCAT, and AMVs was tested for both seasons. Figure 8 shows the percentage change of the root mean square (rms) difference between forecast and observations for the forecast fields used in the calculation of the NWP index. The observations used in this comparison come from radiosondes, AMDAR measurements and satellite winds. A skill score is calculated by normalising the forecast rms error against the persistence rms error. These skill scores are then combined using different weights to form a single index representing the total impact of the change. The change in the NWP index was +0.13 for the February/March OSE was and +0.22 for the July/August experiment. This is for a roughly 20% increase in the number of IASI observations. The scale of this change is compared to the effect of removing both IASI instruments and removing all MetOp-B instruments in table 1. Further discussion of the first season results may be found in Cameron (2013b).

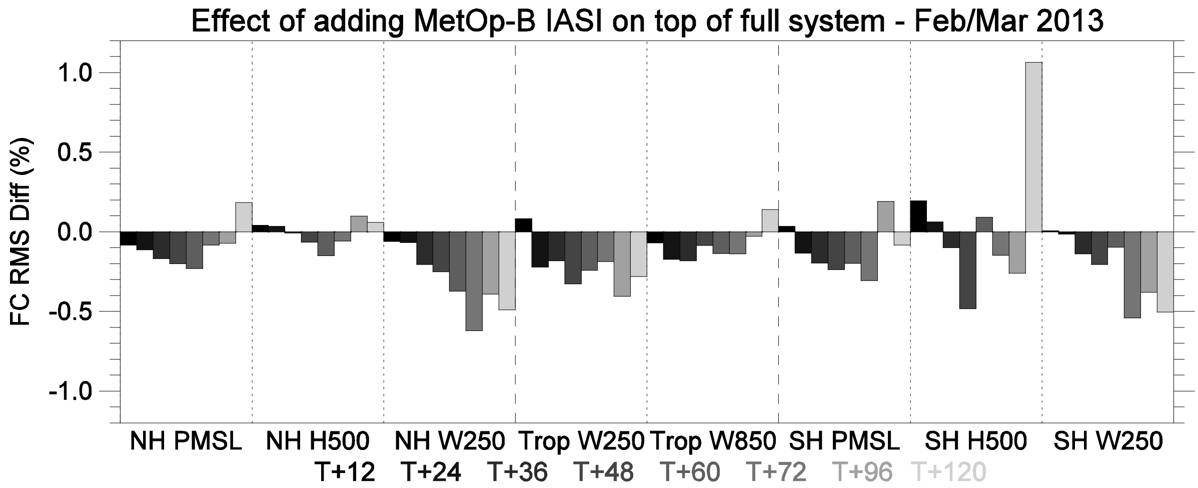

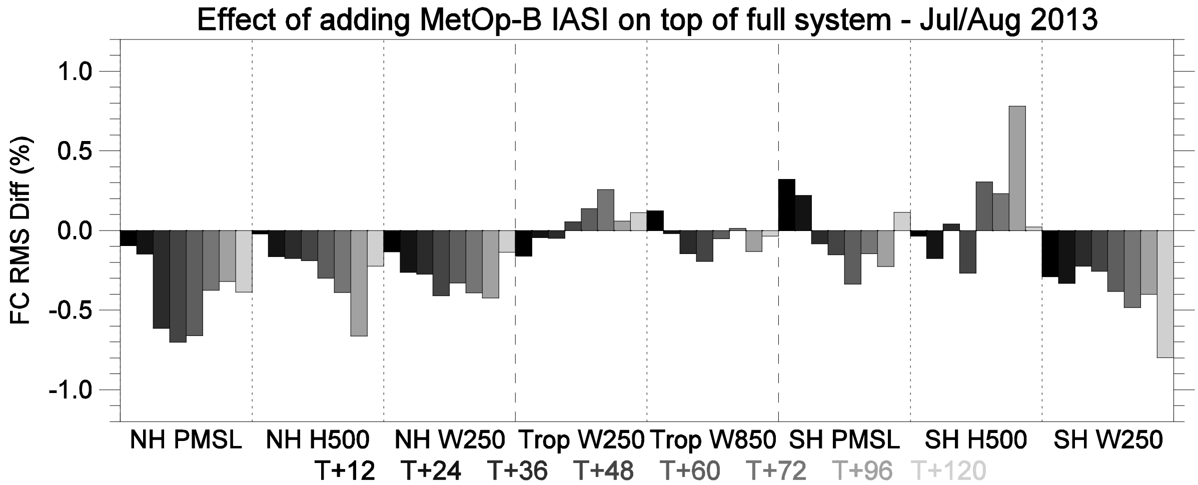

Figure 8: **The percentage change of the RMS difference between forecast and observations for the forecast fields used in the calculation of the NWP index.**

Season	**Number of days**	**Experiment**	**Control**	**NWP Index change**
Feb/Mar 13	52	Full system	Full system minus MetOp-B IASI	+0.13
Feb/Mar 13	34	Full system	Full system minus both IASIs	+1.04
Feb/Mar 13	52	Full system	Full system minus all MetOp-B instruments	+0.27
Jul/Aug 13	45	Full system	Full system minus MetOp-B IASI	+0.22
Jul/Aug 13	45	Full system	Full system minus both IASIs	+0.77

Table 1: **The change in the NWP index for various OSEs.**

Forecast sensitivity to MetOp-B IASI

Statistics on the sensitivity of the forecast to observations were collected for the period 23 March–25 April 2013. The method used is described in Lorenc and Marriott (2013). The experiment included hybrid assimilation, but with the forecasts run at N320 rather than N512 resolution. Figure 9 shows the impact of each observation type for a moist energy norm. It can be seen that the impact of MetOp-B IASI is about 20% of that of MetOp-A IASI, consistent with the ratio of the numbers of observations assimilated. Plots of the impact per channel and impact per sounding (not shown here) show very similar values for MetOp-A and MetOp-B IASI, strongly suggesting that MetOp-B IASI is delivering the expected impact.

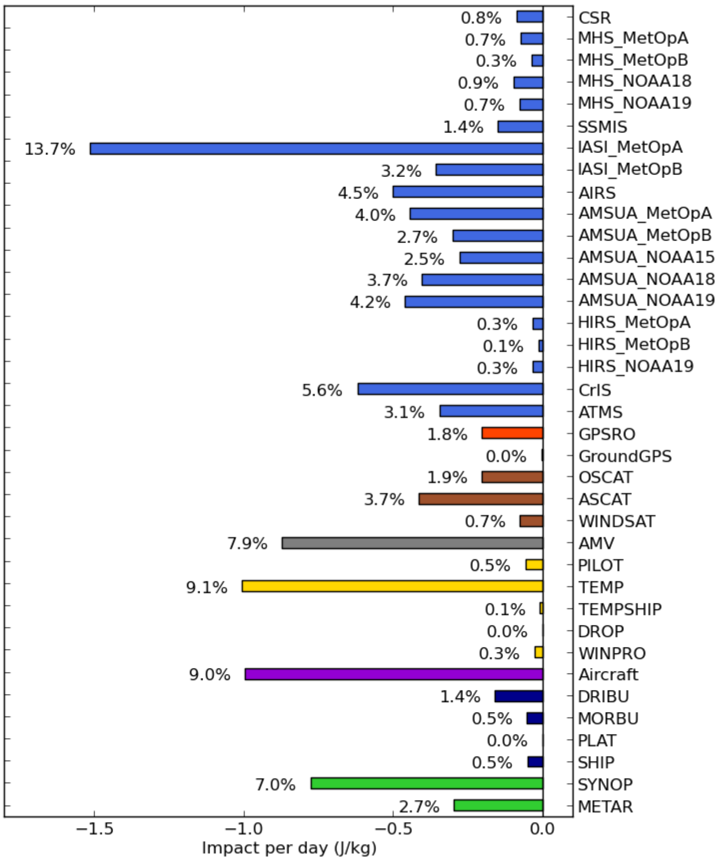

Figure 9: **The mean impact per day of different observation types as derived from a forecast sensitivity experiment.**

CONCLUSIONS

From comparison of MetOp-A and MetOp-B observed minus background radiances, the bias of MetOp-B is the same as MetOp-A to less than 0.1K. The Standard deviation of observed minus background is up to 10-15% less for MetOp-B than for MetOp-A in some channels. Inter-FOV biases are smaller for MetOp-B than for MetOp-A.

Assimilating MetOp-B IASI in a system that already includes MetOp-A IASI has a positive impact on the forecast for both seasons tested. There is a 20% increase in the number of IASI observations assimilated, there is improved data coverage, and the system will be more robust to interruptions in the flow of data. A forecast sensitivity experiment for the period 23 March–25 April 2013 indicates that the impact per observation for MetOp-B IASI is very similar to that of MetOp-A IASI. This is good evidence that MetOp-B IASI is delivering the expected impact.

REFERENCES

Cameron, J. R. N., (2013a) Comparison of locally received MetOp-B IASI data with global MetOp-A IASI data. Forecasting Research Technical Report No: 575, Available from: http://www.metoffice.gov.uk/media/pdf/s/b/FRTR575.pdf

Cameron, J. R. N., (2013b) Initial assessment of the impact of MetOp-B IASI. Forecasting Research Technical Report No: 579, Available from: http://www.metoffice.gov.uk/media/pdf/n/9/FRTR579.pdf

Lorenc, A. C. and Marriott, R. T. (2013), Forecast sensitivity to observations in the Met Office Global numerical weather prediction system. Q.J.R. Meteorol. Soc.. doi: 10.1002/qj.2122